An electrochemical intraocular drug delivery device

Po-Ying Li [a], Jason Shih [b], Ronalee Lo [a], Saloomeh Saati [c], Rajat Agrawal [c],
Mark S. Humayun [c], Yu-Chong Tai [b], Ellis Meng [a],*

[a] *Biomedical Microsystem Laboratory, University of Southern California, USA*
[b] *Caltech Micromachining Laboratory, California Institute of Technology, USA*
[c] *Keck School of Medicine, University of Southern California, USA*

Abstract

A microelectromechanical systems (MEMS) drug delivery device is investigated for the treatment of incurable ocular diseases. Unlike conventional ocular drug delivery devices, this MEMS device is capable of being refilled, features electronic control of the drug regimen, and enables targeted intraocular drug delivery. The refillable design permits long-term drug therapy and avoids repetitive surgeries. Electronic control of dosing is achieved by using electrolysis-actuated pumping to deliver pharmaceuticals directly to the intraocular space. A flexible Parylene transscleral cannula allows targeted delivery to tissues in both the anterior and posterior segments of the eye. This electrochemically driven drug delivery device was demonstrated to provide flow rates suitable for ocular drug therapy (pL/min to µL/min). Both continuous and bolus drug delivery modes were performed to achieve accurate delivery of a target volume of 250 nL. An encapsulation packaging technique was developed for acute surgical studies and preliminary *ex vivo* drug delivery experiments in porcine eyes were performed.
© 2007 Elsevier B.V. All rights reserved.

Keywords: Drug delivery device; Electrolysis pump; Refillable reservoir; Intraocular

1. Introduction

Intraocular diseases such as retinitis pigmentosa, age-related macular degeneration, diabetic retinopathy, and glaucoma are presently incurable and affect millions worldwide [1]. Disease progression and lack of treatment may lead to blindness. Drug therapy is currently the most effective treatment, however, conventional administration methods are limited in efficacy. To successfully treat these diseases, pharmaceuticals must penetrate the protective physiological barriers of the eye such as the cornea, sclera, and the blood–retina barrier and target difficult-to-reach intraocular tissues such as the ciliary body, retina, and angle [2]. The goal of precise and targeted delivery to these tissues remains elusive with modern treatments.

Conventional ocular drug delivery therapies include oral drugs, eye drops, and intraocular injections. Oral and topical methods require large overdoses to reach therapeutic levels in the intraocular space. It has been shown that less than 5% of the applied medication is able to penetrate physiological barriers [3]. Severe systemic side effects may also result. To overcome physical barriers to ocular drug delivery, periocular or intraocular approaches are necessary. Intraocular injections directly deliver pharmaceuticals to intraocular tissues but require repeated injections (as frequent as one to three per week) for treating chronic diseases and may contribute to dose-related side effects [4]. Many of these methods exhibit low patient compliance.

Drug delivery devices provide advanced ocular drug therapy. Sustained-release implants (biodegradable or non-biodegradable) allow continuous release of drug over extended periods of time [4,5]. These devices contain a fixed charge of drug specially formulated for release at a fixed rate; after implantation, it is not possible to change the drug, its concentration, or its release rate. In addition, these devices cannot be refilled. Once the drug is expended, the implant must be surgically removed and replaced. Sustained-release implants are limited by safety concerns and lack of precision in the erosion rate [6].

Implantable pump systems have not been present historically in ocular drug delivery due to large size and mediocre performance [5]. However, with MEMS technology, miniaturized devices having precise delivery in either bolus or continuous

---

* Corresponding author.
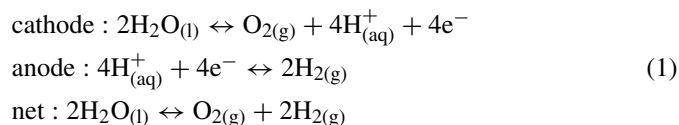 *E-mail address:* ellismen@usc.edu (E. Meng).

mode are possible. The advantages of MEMS fabrication for producing miniaturized and efficient drug delivery systems have already been realized for insulin delivery and delivery of bioactive compounds to neural tissue [7–9]. Due to the limitations of traditional methods of treatment for ocular diseases, there is a need for MEMS ocular drug delivery systems that are capable of targeted delivery to interior tissues, refillable for long-term use, and automated to address patient compliance.

We previously demonstrated the feasibility of MEMS for implantable intraocular drug delivery in a passive, or unpowered, device [10]. This device contained a drug reservoir attached to a flexible check-valved cannula that was directed through the eye wall by means of a small surgical incision. This configuration allowed drug to be delivered directly into the eye and reach intraocular tissues in the vicinity of the cannula outlet. To deliver drug into the eye, the device was actuated by manually depressing the drug reservoir. This action generated an overpressure in the reservoir which in turn caused a check valve in the cannula to open and allow drug to enter the intraocular space. The reservoir was emptied over time by repeated dosing by manual actuation. Upon depletion of the reservoir, the drug reservoir was refilled by puncturing the reservoir wall with a syringe needle and emptying the syringe into the reservoir. This was the first refillable ocular drug delivery device which extends device lifetime in the patient and provides long-term therapy. To achieve variable delivery rates and the ability to select either bolus or continuous delivery, an active device having electrochemically driven drug delivery was investigated [11].

2. Theory

The electrolysis of water results in the phase transformation of liquid to gas. This reaction is utilized here to replace the manual actuation in the passive device. The electrochemical production of hydrogen and oxygen gases generates sufficient pressure within the drug reservoir to deliver drug into the eye (Fig. 1). Electrolysis actuation has attracted attention among other forms of microactuation for its low power consumption, simple construction, and ability to generate large displacements [12]. Electrolysis actuation as an effective means for pumping fluids is well established in microfluidics [13–15].

The electrolysis of water can be summarized by the following reactions:

Fig. 1. Cross-section of the ocular drug delivery device depicting electrochemical pumping of drug into the eye.

$$\text{cathode} : 2H_2O_{(l)} \leftrightarrow O_{2(g)} + 4H^+_{(aq)} + 4e^-$$
$$\text{anode} : 4H^+_{(aq)} + 4e^- \leftrightarrow 2H_{2(g)} \qquad (1)$$
$$\text{net} : 2H_2O_{(l)} \leftrightarrow O_{2(g)} + 2H_{2(g)}$$

The net result is the production of oxygen and hydrogen gas which contributes to a volume expansion of about a thousand times greater than the starting volume of water. This gas evolution process proceeds even in a pressurized environment; it has been reported that the maximum pressure at which the reaction can occur is 200 MPa [16]. Electrolysis requires four electrons in order to convert two water molecules into three gas molecules (two hydrogen and one oxygen). To drive gas generation and thus pumping, current control is the preferred biasing scheme as there is a direct correlation of the applied current to the generated gas volume and the fluid flow rate. The theoretical pump rate ($q_{\text{theoretical}}$ in m^3/s) at atmospheric pressure for current-controlled electrolysis pumping is given by

$$q_{\text{theoretical}} = \frac{3}{4}\frac{i}{F}V_m \qquad (2)$$

where i is current (in A), F the Faraday's constant (96.49×10^{-3} C/mol), and V_m is the molar gas volume at $25\,^{\circ}C$ and atmospheric pressure ($24.7 \times 10^{-3}\,m^3/mol$). The theoretical generated or dosed gas volume ($V_{\text{theoretical}}$ in m^3) can be determined by

$$V_{\text{theoretical}} = q_{\text{theoretical}}t \qquad (3)$$

where t is duration (in s) for which the current is applied.

The efficiency (η) of an electrolysis actuator as a pump can be defined as [15]

$$\eta = \frac{V_{\text{experimental}}}{V_{\text{theoretical}}} \qquad (4)$$

where $V_{\text{experimental}}$ is the actual volume of the generated hydrogen and oxygen gases. Efficiency in electrochemical systems is a complex function of several parameters that have been categorized by Bard and Faulkner. The variables include electrode design (material, surface area, geometry, and surface conditions), mass transfer conditions (transport mode, surface concentration, and adsorption), external parameters (temperature, pressure, and time), electrolysis solution (bulk concentration of electroactive species, concentration of other species, and solvent), and electrical parameters (potential, current, and quantity of electricity) [17].

3. Design

The drug delivery device consists of an electrolysis pump, drug reservoir, and transscleral cannual (Fig. 2). The electrolysis pump consists of two interdigitated platinum electrodes immersed in an electrolyte. This electrode geometry improves pumping efficiency by reducing the current path through the solution which also serves to lower the heat generation [18]. When current or voltage is applied, with the drug as an electrolyte, electrolysis of water in the drug at the electrodes produces oxygen and hydrogen gases. The gases generated result
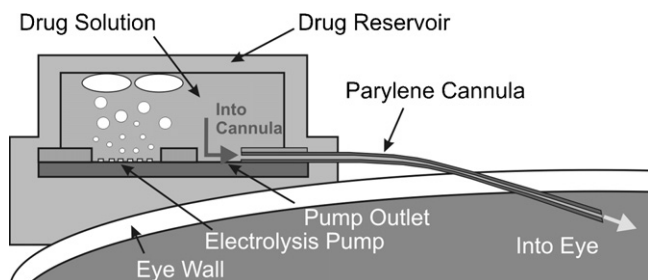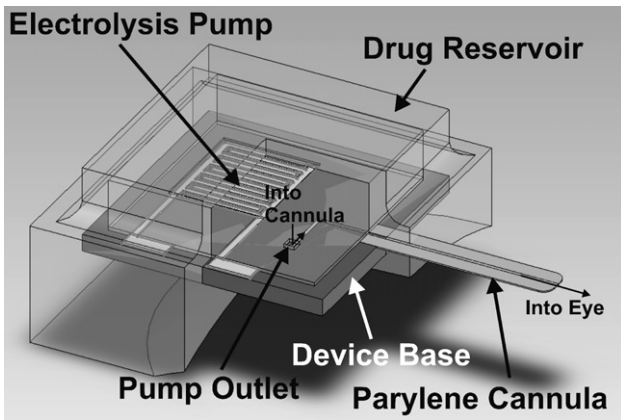
Fig. 2. Schematic diagram illustrating the components of the drug delivery device. The arrows follow the drug flow path from the reservoir through the Parylene cannula.
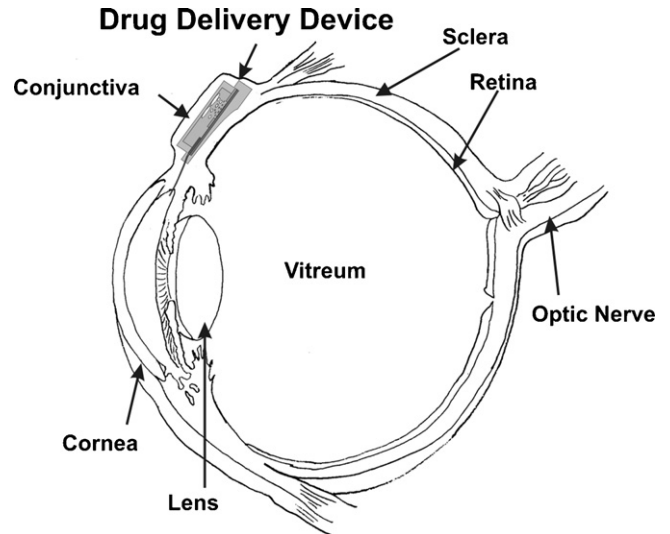

Fig. 3. Conceptual illustration of the implanted ocular drug delivery device. The device is implanted under conjunctiva with the cannula is directed through a limbal incision into the anterior segment of eye.

in an internal pressure increase in the sealed reservoir which causes drug to be delivered through the cannula and into the eye. Electrolysis is a reversible process and ceases when the applied bias is turned off. This allows the gradual recombination of hydrogen and oxygen to water.

Drug is stored in a reservoir integrated on top of the electrolysis pump. This reservoir was casted in silicone rubber (Sylgard 184, Dow Corning, Midland, MI) and assembled on top of the pump chip by using an encapsulation technique. Previously, we demonstrated that silicone rubber is suitable as a refillable reservoir material; thin silicone membranes were able to sustain multiple punctures from a non-coring syringe needle required to refill the reservoir. Silicone rubber membranes were able to reseal repeatedly without leakage after removal of the needle and remained leak-free even after the application of differential pressure across the membrane [10].

A flexible transscleral cannula is connected to the pump chamber through a small port. This layout traps generated gases inside the reservoir while allowing pumped drug to escape into the eye (Figs. 2–3). This cannula was surgically inserted through a small incision in the eye wall and was directed into either the anterior or posterior segment of the eye. Targeted drug delivery can be achieved by placing the cannula outlet in the vicinity of the desired treatment site. Parylene C (Specialty Coating Systems Inc., Indianapolis, IN) was selected as the cannula material for its mechanical strength, biocompatibility, and ease of integration. It is a USP Class VI material suitable for the construction of implants and is well established as a MEMS material [19].

The drug delivery system is assembled from two separately fabricated components: (1) the pump chip with an integrated cannula and (2) the reservoir. The pump/cannula chip was fabricated using conventional silicon micromachining and the reservoir by the casting of silicone rubber against a master mold.

4. Fabrication

The fabrication process of the pump and cannula chip (Fig. 4) starts with a thermally oxidized silicon substrate (5000 Å)

(Fig. 5A). LOR 3B (MicroChem Corp., Newton, MA) was spun on at 3 krpm followed by AZ 1518 (AZ Electronic Materials, Branchburg, NJ) at 3 krpm. Ti/Pt (200/2000 Å) was e-beam evaporated and patterned by lift-off in ST-22 photoresist stripper (ATMI, Danbury, CT) to define the interdigitated electrodes of the electrolysis pump (Fig. 5B). A second lithography step was performed (AZ 1518 at 3 krpm) to define the cannula footprint. The oxide layer was etched using buffered hydrofluoric acid to expose the silicon below. The photoresist was stripped then the exposed silicon was roughened by two cycles of XeF_2 etching (Fig. 5C). The first sacrificial photoresist layer (AZ 4620 spun at 2.75 krpm and hard baked to yield a 5 μm thick layer) was applied to facilitate release of the cannula from the substrate (Fig. 5D). The first Parylene C layer (7.5 μm) forming the bottom of the cannula was deposited followed by thermal evaporation of 2000 Å thick Cr etch mask. Following lithogra-
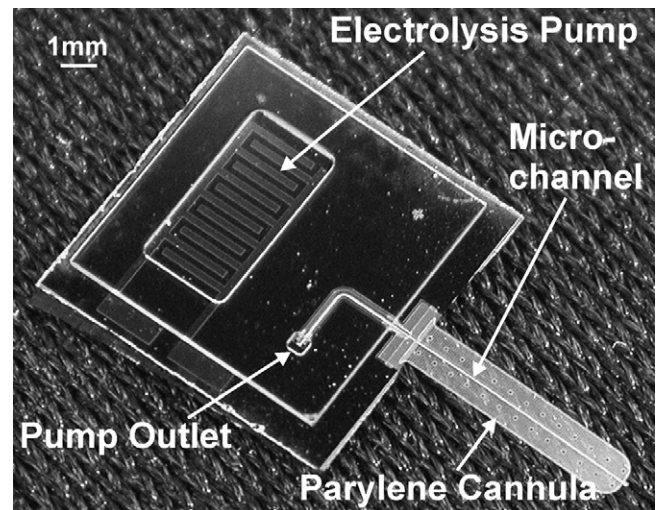

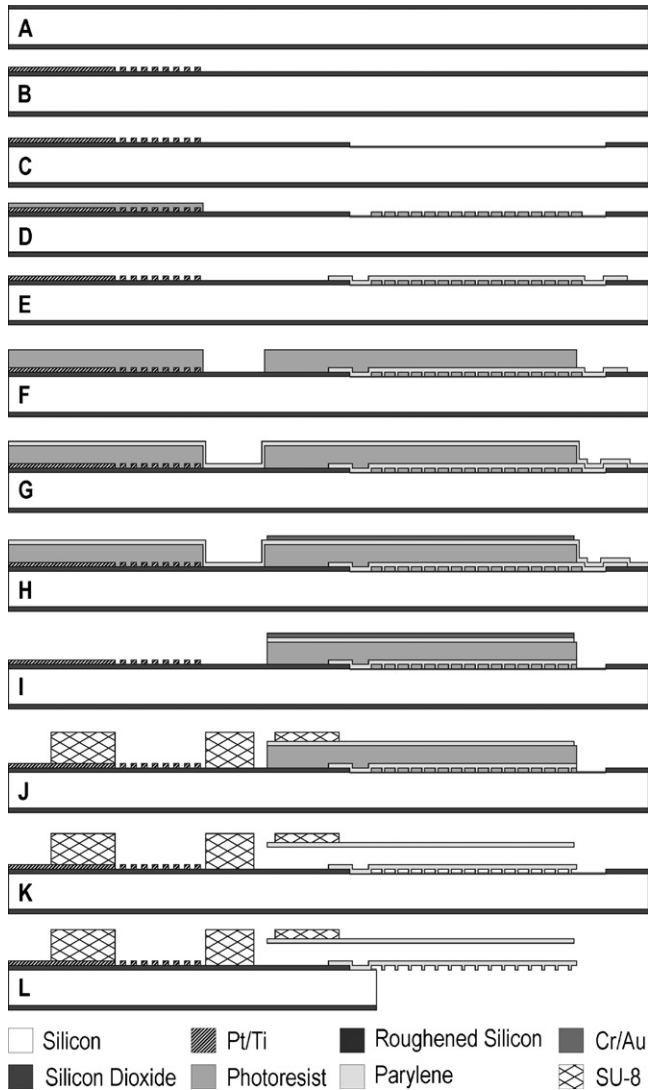Fig. 4. Fabricated pump and cannula chip (1 mm wide cannula with an embedded microchannel measuring 100 μm $\times$ 25 μm $\times$ 5 mm).

Fig. 5. Simplified fabrication process for the pump/cannula chip.

were released manually by gently lifting them off the substrate. Finally, individual dies were separated and the remaining silicon beneath each cannula was removed by scribing and breaking it off (Fig. 5L).

4.1. Device assembly and surgical packaging

Additional packaging and assembly were required for implementation of the device in surgical experiments. The pump chip containing the electrolysis actuator and cannula was combined with the drug reservoir and electrical wiring for supplying current to the electrolysis electrodes. This assembly is shown in Fig. 6. First, electrical wires were bonded to the electrolysis electrode contact pads with conductive epoxy (Ohmex-AG, Transene Company Inc., Danvers, MA). The epoxy was cured at 150 °C for 15 h under vacuum. The pump chip and drug reservoir were then assembled by using an encapsulation technique based on silicone soft lithography [20,21] (Fig. 7). A silicone spacer (Sylgard 184, Dow Corning, Midland, MI) was casted against a stainless steel sphere (17.5 mm in diameter) to adapt the planar device to fit comfortably against the curvature of the eye (Fig. 7A). Silicone rubber was mixed using a 10:1 base-to-curing agent ratio (AR-250 Hybrid Mixer, Thinky Corp., Tokyo, Japan) and partially cured (65 °C for 20 min). The sphere mold was removed and the resulting crater was filled with wax (Parowax, Roswell, GA) (Fig. 7B and C). A drug reservoir was prepared by casting silicone rubber against a conventionally machined acrylic mold (partially cured at 65 °C for 20 min) (Fig. 7D and E). The reservoir has internal dimensions of 6 mm × 6 mm × 1.5 mm which provides a maximum of 54 μL of drug storage. The silicone reservoir was aligned

phy (AZ 4620 at 500 rpm), the Cr was etched in CR-7 (Cyantek, Fremont, CA) then the photoresist was stripped. The Parylene layer was then patterned in an oxygen plasma and the Cr etch mask was removed (CR-7) (Fig. 5E). A second photoresist sacrificial layer was deposited (AZ 4620 spun at 450 rpm and hard baked to yield a 25 μm thick layer) to define the channel height (Fig. 5F). A second Parylene layer (7.5 μm) was deposited to complete the cannula (Fig. 5G). To define the cannula from the Parylene/photoresist/Parylene sandwich, Ti/Au (200/2000 Å) was deposited as an etch mask. The etch mask was patterned (AZ 4620 spun at 425 rpm) and etched first with Au Etchant TFA (Transene Company Inc., Danvers, MA) and then 10% HF (Fig. 5H). Finally, the sandwich was etched in oxygen plasma and the masking layer was stripped (Au Etchant TFA and 10% HF) (Fig. 5I). Following the etch, the entire wafer was cleaned in 5% HF dip and by exposure to oxygen plasma. SU-8 50 (MicroChem Corp., Newton, MA) was spun at 2200 rpm resulting in a 70 μm thick layer after post-baking (Fig. 5J). The sacrificial photoresist was removed by dissolving in a 40 °C acetone solution for 1 day (Fig. 5K). The individual cannulae
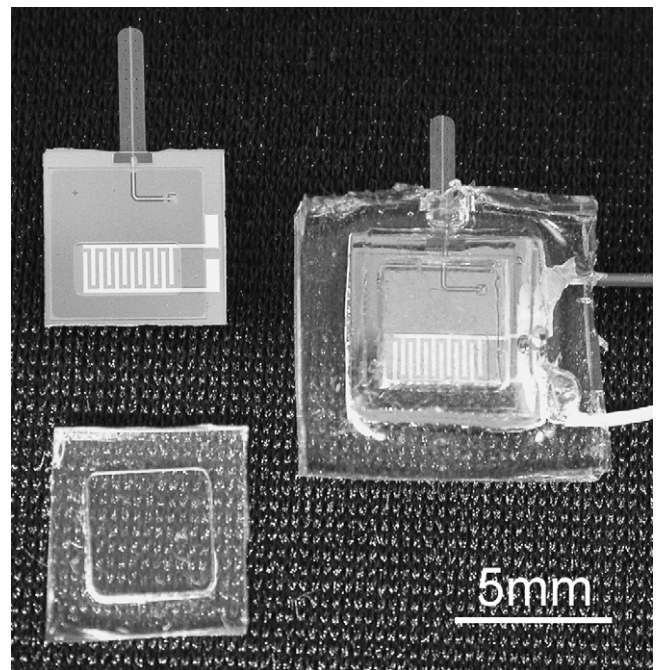

Fig. 6. Pump and cannula chip (upper left), silicone drug reservoir (lower left), and packaged drug delivery device with attached wires for electrolysis actuation (right).
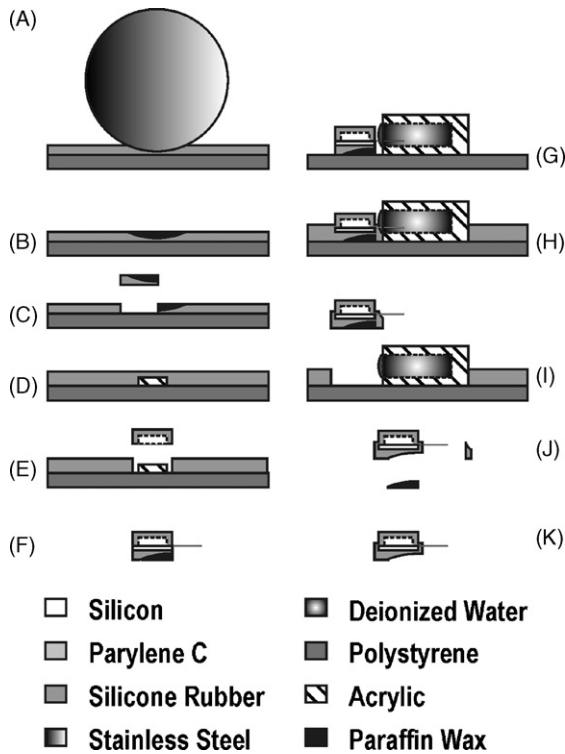
Fig. 7. Fabrication process detailing steps for device packaging.

Fig. 8. Schematic diagram of the flow rate testing apparatus.

to the pump/cannula chip and silicone spacer (Fig. 7F). Then the Parylene cannula was immersed in deionized water which serves as a mask to prevent coating by silicone rubber during the encapsulation step (Fig. 7G). This assembly process exploits the hydrophobicity of silicone rubber. The stack was immersed in silicone prepolymer and cured at room temperature for 24 h (Fig. 7H). Finally, extraneous silicone material was removed from the device to complete the assembly process (Fig. 7I and K).

5. Experimental methods

5.1. Bench-top testing

To investigate the performance of the electrolysis pump, experiments examining continuous delivery, bolus delivery, pump efficiency, gas recombination, and backpressure were conducted. For these tests, a custom testing apparatus was laser-machined (Mini/Helix 8000, Epilog, Golden, CO) in acrylic. The experimental setup consisted of a computer-controlled CCD camera (PL-A662, PixeLINK, Ottawa, Canada) for collecting flow data from a calibrated micro-pipette (Accu-Fill 90, Becton, Dickinson and Company, NJ) connected to the output port of the test fixture (Fig. 8). Testing was performed using dyed deionized water as the electrolyte. The electrolysis was sustained under constant current conditions (50 μA to 1.25 mA) for continuous delivery operation. The pump efficiency associated with these results was calculated from (4). The relationship between efficiency and recombination of hydrogen and oxygen to water was determined.
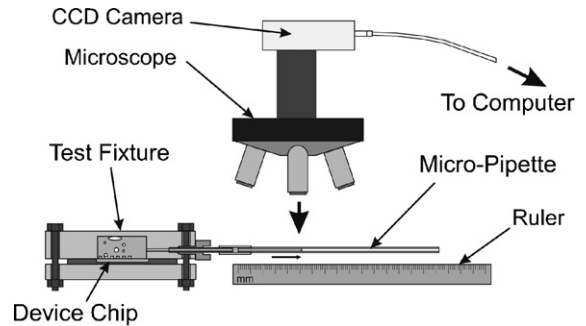
Bolus delivery was also examined. A constant current pulse (0.5, 1.0, and 1.5 mA) was applied for 1, 2, and 3 s. Repeated trials were performed ($n = 4$) to obtain the average dosed volume. Normal intraocular pressure (IOP) ranges from 5 to 22 mmHg (15.5 ± 2.6 mmHg (mean $\pm$ S.D.)) [22]. Values outside this range correspond to abnormal intraocular pressure which is a characteristic of glaucoma (>22 mmHg). Thus, it is necessary to characterize pump performance under these physiologically relevant conditions. The experimental setup in Fig. 8 was modified for this analysis by connecting a water column to the outlet of the micro-pipette. Backpressure was applied to the drug delivery device by adjusting the height of the water column. Data was collected for backpressures corresponding to normal IOP (20 mmHg) and abnormal IOP (0 and 70 mmHg).

5.2. Surgical testing

The prototype drug delivery devices were implanted in enucleated porcine eyes. Preliminary *ex vivo* surgical modeling in enucleated porcine eyes is necessary to prepare for device demonstration *in vivo*. The operation of each surgical device was tested prior to the surgical experiment to check for clogs in the cannula and to verify the integrity of the electrical connections. The drug reservoir was filled with dyed deionized water then the reservoirs were manually depressed which generates sufficient pressure to expel the fluid from the reservoir. A second test was conducted to verify operation of the electrolysis pump by connecting to an external power supply and driving fluid from the reservoir by electrolysis pumping. An enucleated porcine eye was prepared for the surgical study and a limbal incision was made (between the cornea and sclera). The cannula was implanted through the incision into the anterior chamber of the eye (Fig. 9). The enucleated porcine eye was pressurized to 15 mmHg by using an infusion line. Constant current (0.5 mA) was applied for 1 min. The device was surgically removed after the experiment.

6. Results and discussion

The electrolysis pump was operated at flow rates in the pL/min to μL/min range using driving currents from 5 μA to 1.25 mA (Fig. 10A–B). The highest flow rate was 7 μL/min for 1.25 mA and the lowest was 438 pL/min at 5 μA. Both data sets were corrected to compensate for the evaporation of fluid during
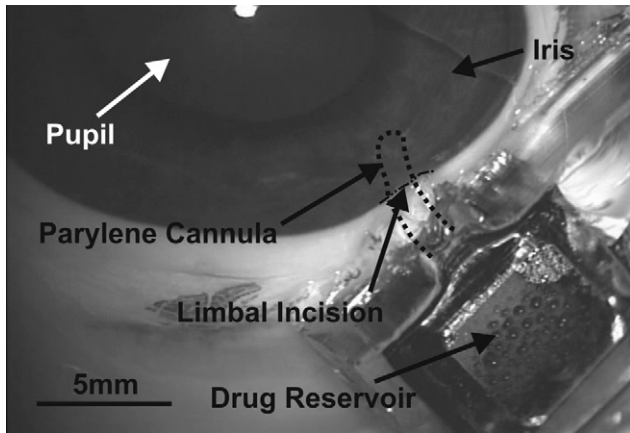
Fig. 9. *Ex vivo* testing of the device in porcine eye showing the electrolysis driven delivery of dyed deionized water into anterior chamber.

Fig. 11. Bolus delivery of 250 nL doses using current pulses.

testing. Flow rates below about 2 μL/min are preferred for ocular drug delivery. This is consistent with naturally occurring flow rates in the eye; the ciliary body of the eye produces aqueous humor at 2.4 ± 0.6 μL/min in adults [22]. As current decreases, it was observed that pumping efficiency, which ranged from 24% to 49%, also decreased (Fig. 10C). These efficiency values are consistent with those reported for other electrochemical pumps [15]. Electrolysis-driven pumping efficiency was affected by the competitive recombination of hydrogen and oxygen gases to water. This effect was further accelerated by exposure to the platinum electrolysis electrodes which serve to catalyze the
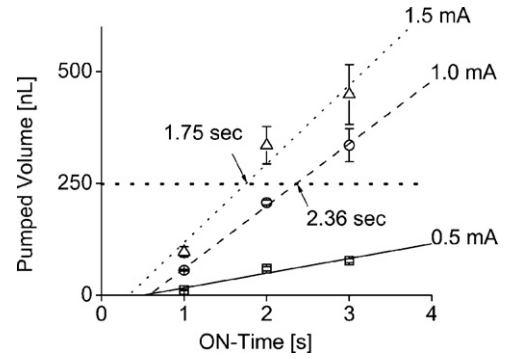
recombination reaction. In Fig. 10D, a typical accumulated volume curve is shown that illustrates the effect of recombination after the applied current is turned off. The measured recombination rate was 62 nL/min.

Bolus delivery mode was also evaluated (Fig. 11). If the desired dosing regimen requires 250 nL per dose, this volume can be obtained by driving the pump for a short duration that is associated with the magnitude of the applied current. For example, a 1.0 mA driving current will dose 250 nL in 2.36 s and, for 1.5 mA current, the pulse time can be set as 1.75 s. Under normal operation in the eye, the drug delivery device will experience a backpressure equivalent to the IOP of the eye. Bench-top experiments indicated that the pump was able to supply sufficient drug flow (up to 1500 nL/min) over the range of normal
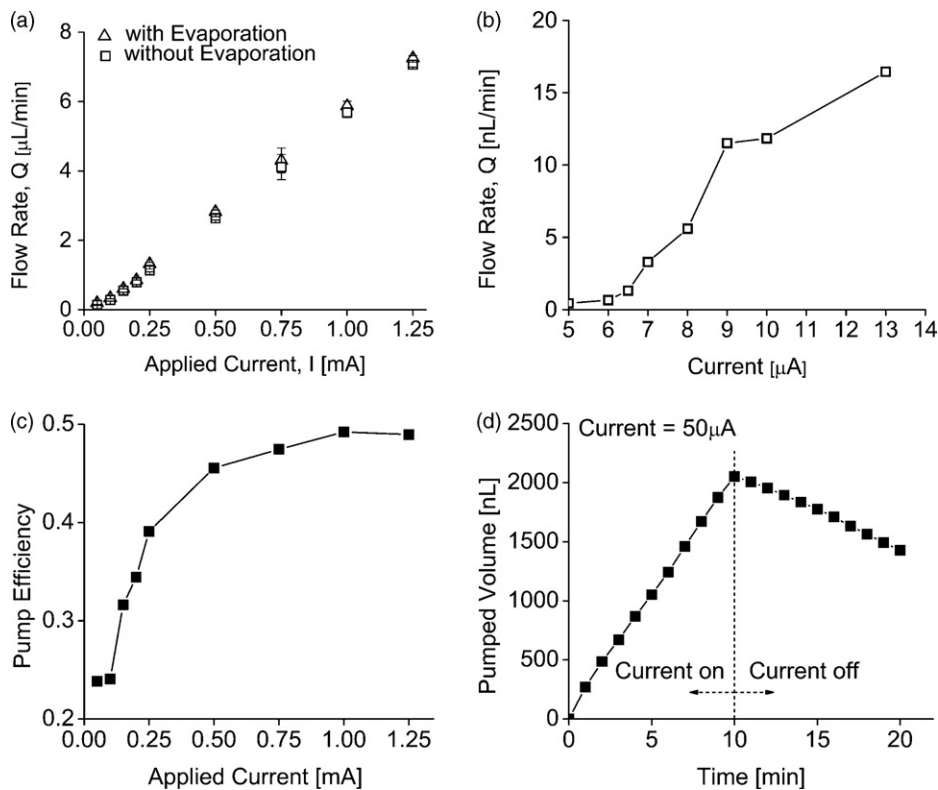

Fig. 10. (a) Current-controlled flow delivery after evaporation compensation (mean ± S.E., $n = 4$). The calibrated water evaporation rate in the micro-pipette is ~30 nL/min. (b) Low flow rate operation of the drug delivery device. (c) Pump efficiency calculated from flow delivery data. (d) Typical gas recombination observed in the drug delivery device. Current (50 μA) was applied for 10 min and then turned off.
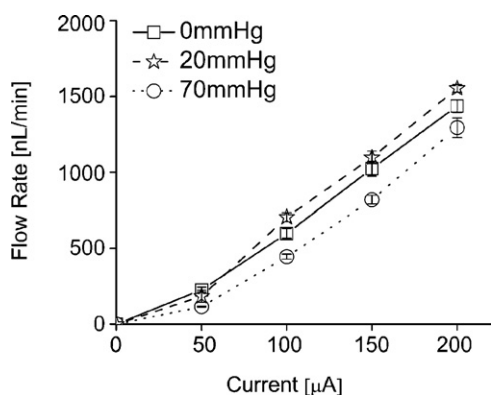
Fig. 12. Flow performance under physiological back pressures (mean ± S.E., $n = 4$).

and abnormal IOP equivalent backpressures (Fig. 12). The flow rates subjected to abnormal IOPs varied by approximately 30% compared to normal IOP values.

Our device has demonstrated the flexibility to achieve pL to μL/min flow ranges suitable for a wide range of intraocular pharmacological therapies. For example, drugs used in current sustained-release implants for treating conditions that affect ocular tissues in the difficult-to-reach posterior segment of the eye are fluocinolone acetonide and ganciclovir. A fluocinolone acetonide implant for treating posterior uveitis was demonstrated to release drug at 0.6 μg/day for over 1000 days [23]. A ganciclovir implant for treating cytomegalovirus retinitis released at 48 μg/day for over 190 days [24]. In our electrolysis-based delivery system, ~10% by weight liquid drug formulation with an estimated solution density of 1.0 g/cm^3 will be used. For release rates corresponding to 0.6–48 μg/day, the respective drug delivery rates of 6.5–520 nL/day are required and fall within the performance range of our device. Extensive animal testing is required to fully assess the pharmacological efficacy and safety of these flow ranges and is planned.

Initial surgical results yielded promising results in enucleated porcine eyes. Following removal of the device after the surgical experiment, post-surgical examination of the eye through an ophthalmic operating microscope revealed a small spot of dye located above the iris near the position of the cannula tip indicating that dye was delivered into the eye.

7. Conclusion

An electrochemically driven implantable MEMS drug delivery device featuring integration of a pump, drug reservoir, and transscleral cannula was prototyped and tested. Bench-top testing results demonstrated that this electrochemically driven micropump can provide a wide operation range (pL/min to μL/min) suited for ocular drug delivery treatment of chronic diseases. Drug delivery against opposing backpressures equivalent to normal and elevated intraocular pressures was also demonstrated. Preliminary *ex vivo* testing was performed demonstrating the feasibility of this device for ocular drug delivery. Future work will focus on optimizing the electrolysis pump and the integration of a check valve to prevent back flow of intraocular fluids into the device through the cannula. Operation with ophthalmic drugs and *in vivo* demonstration are also planned.

Acknowledgements

References

[1] D.H. Geroski, H.F. Edelhauser, Drug delivery for posterior segment eye disease, Invest. Ophthalmol. Vis. Sci. 41 (2000) 961–964.
[2] N. Acharya, L. Young, Sustained-release drug implants for the treatment of intraocular disease, Int. Ophthalmol. Clin. 44 (2004) 33–39.
[3] D.C. Metrikin, R. Anand, Intravitreal drug administration with depot devices, Curr. Opin. Ophthalmol. 5 (1994) 21–29.
[4] S. Lee, P. Yuan, M.R. Robinson, Ocular implants for drug delivery, Encyclopedia of biomaterials and biomedical engineering (2004) 1105–1119.
[5] J. Ambati, E.S. Gragoudas, J.W. Miller, T.T. You, K. Miyamoto, F.C. Delori, A.P. Adamis, Transscleral delivery of bioactive protein to the choroid and retina, Invest. Ophthalmol. Vis. Sci. 41 (2000) 1186–1191.
[6] V.V. Ranade, M.A. Hollinger, Drug Delivery Systems, 2nd ed., CRC Press, Boca Raton, 2004, p. 448.
[7] A.C.R. Grayson, R.S. Shawgo, Y.L. Li, M.J. Cima, Electronic MEMS for triggered delivery, Adv. Drug Deliv. Rev. 56 (2004) 173–184.
[8] S.Z. Razzacki, P.K. Thwar, M. Yang, V.M. Ugaz, M.A. Burns, Integrated microsystems for controlled drug delivery, Adv. Drug Deliv. Rev. 56 (2004) 185–198.
[9] B. Ziaie, A. Baldi, M. Lei, Y.D. Gu, R.A. Siegel, Hard and soft micromachining for bioMEMS: review of techniques and examples of applications in microfluidics and drug delivery, Adv. Drug Deliv. Rev. 56 (2004) 145–172.
[10] R. Lo, K. Kuwahara, P.-Y. Li, R. Agrawal, M.S. Humayun, E. Meng, A passive refillable intraocular MEMS drug delivery device, in: Proceedings of the 2006 International Conference on Microtechnologies in Medicine and Biology, Okinawa, Japan, 9–12 May, 2006, pp. 74–77.
[11] P.-Y. Li, J. Shih, R. Lo, B. Adams, R. Agrawal, S. Saati, M.S. Humayun, Y.-C. Tai, E. Meng, An electrochemical intraocular drug delivery device, in: Proceedings of the 20th IEEE International Conference on Micro Electro Mechanical Systems, Kobe, Japan, 21–25 January, 2007, pp. 15–18.
[12] C.R. Neagu, J.G.E. Gardeniers, M. Elwenspoek, J.J. Kelly, An electrochemical microactuator: principle and first results, J. Microelectromech. Syst. 5 (1996) 2–9.
[13] S. Bohm, B. Timmer, W. Olthuis, P. Bergveld, A closed-loop controlled electrochemically actuated micro-dosing system, J. Micromech. Microeng. 10 (2000) 498–504.
[14] D. O'Keefe, C. Oherlihy, Y. Gross, J.G. Kelly, Patient-controlled analgesia using a miniature electrochemically driven infusion-pump, Br. J. Anaesth. 73 (1994) 843–846.
[15] J. Xie, Y.N. Miao, J. Shih, Q. He, J. Liu, Y.C. Tai, T.D. Lee, An electrochemical pumping system for on-chip gradient generation, Anal. Chem. 76 (2004) 3756–3763.
[16] C.G. Cameron, M.S. Freund, Electrolytic actuators: alternative, high-performance, material-based devices, Proc. Natl. Acad. Sci. U.S.A. 99 (2002) 7827–7831.
[17] A.J. Bard, L.R. Faulkner, Electrochemical Methods—Fundamentals and Applications, 2nd ed., John Wiley & Sons Inc., Hoboken, 2001, p. 19.
[18] C. Belmont, H.H. Girault, Coplanar interdigitated band electrodes for electrosynthesis. Part 2. Methoxylation of furan, J. Appl. Electrochem. 24 (1994) 719–724.

[19] E. Meng, P.-J. Chen, D. Rodger, Y.-C. Tai, M. Humayun, Implantable pary-lene MEMS for glaucoma therapy, in: Proceedings of the IEEE Engineering in Medicine and Biology Society Special Topic Conference on Microtech-nology in Medicine and Biology, Oahu, Hawaii, USA, 12–15 May, 2005, pp. 116–119.

[20] M.A. Unger, H.P. Chou, T. Thorsen, A. Scherer, S.R. Quake, Monolithic microfabricated valves and pumps by multilayer soft lithography, Science 288 (2000) 113–116.

[21] H.K. Wu, B. Huang, R.N. Zare, Construction of microfluidic chips using polydimethylsiloxane for adhesive bonding, Lab Chip 5 (2005) 1393–1398.

[22] C.R. Ethier, M. Johnson, J. Ruberti, Ocular biomechanics and biotransport, Annu. Rev. Biomed. Eng. 6 (2004) 249–273.

[23] G.J. Jaffe, R.M. McCallum, B. Branchaud, C. Skalak, Z. Butuner, P. Ashton, Long-term follow-up results of a pilot trial of a fluocinolone acetonide implant to treat posterior uveitis, Ophthalmology 112 (2005) 1192–1198.

[24] D.C. Musch, D.F. Martin, J.F. Gordon, M.D. Davis, B.D. Kuppermann, The Ganciclovir Implant Study Group, Treatment of cytomegalovirus retinitis with a sustained-release ganciclovir implant, N. Engl. J. Med. 337 (1997) 83–90.

Biographies

Po-Ying "Brian" Li received his BS and MS degree in mechanical engineering from Tatung Institute of Technology, Taipei, Taiwan, in 1996 and National Tsing Hua University, Hsinchu, Taiwan, in 2001. He also received an MS degree in materials science from University of Southern California, Los Angeles, in 2004. Currently, he is a PhD candidate in electrical engineering in University of Southern California and member of the Biomedical Microsystems Laboratory. His research activities include drug delivery systems, thermal flow sensors, and electrothermal valves. His broad research interests include BioMEMS, NEMS, solid state physics, microfluidics, microactuators and microsensors, crystallography, solid state physics, materials characterization, solid mechanics, finite element analysis, and bio-electronic packaging.

Jason Shih received his BS from the California Institute of Technology in 2003. He is currently pursuing his PhD in electrical engineering at the same institution. He is a member of the Caltech Micromachining Laboratory and his research interests are in the field of microfluidics. Current projects include chip based liquid chromatography systems, miniature devices for drug delivery, and early detection systems for biowarfare agents.

Ronalee Lo received her BS from Harvey Mudd College in 2001. She worked at a Washington, D.C. based biotechnology consulting firm, BioStar, for one year prior to enrolling at the University of Southern California to pursue a PhD She received a MS in biomedical engineering medical devices and diagnostics from the University of Southern California in 2004. She is currently a member of the Biomedical Microsystems Laboratory and is working toward a PhD in biomedical engineering. Her current research focuses on MEMS drug delivery devices and microfluidic interconnects.

Saloomeh Saati received her MD from IRAN University of Medical Sciences in 1999. She finished her training by completing an ophthalmology residency at Tehran University of Medical Sciences in 2005. Currently, she is a research fellow of ophthalmology at the University of Southern California. She is working on Artificial Retina Project and bioMEMS drug delivery devices. She is a member of Association for Research in Vision and Ophthalmology (ARVO).

Rajat Agrawal received his MD from Nagpur University, India, in 1990. He finished an ophthalmology residency in 1993 from Mahatma Gandhi Memorial Hospital in Bombay, India, and fellowship training in 1995 in Vitreo-Retinal Surgery and Diseases from the Medical Research Foundation in Chennai, India. He is a Diplomate of the National Board in Ophthalmology. Dr Agrawal is currently an Assistant Professor of Ophthalmology at the University of Southern California and Co-Director of Intraocular Implants at the Doheny Eye Institute, Los Angeles. He currently directs the development of Artificial Retinal Prosthesis program. He is also involved in development of new ophthalmic procedures and treatments as well as development of new ophthalmic instruments and drug delivery devices.

Mark S. Humayun received his BS from Georgetown University in 1984, his MD from Duke University in 1989, and his PhD from the University of North Carolina, Chapel Hill in 1994. He finished his training by completing an Ophthalmology residency at Duke and a Fellowship in Vitreoretinal diseases at Johns Hopkins Hospital. Currently, Dr. Humayun is a professor of Ophthalmology, Biomedical Engineering, and Cell and Neurobiology at the University of Southern California. Dr. Humayun is the Director of the National Science Foundation Biomimetic MicroElectronic Systems Engineering Research Center (BMES ERC). He is also the Director for the Department of Energy Artificial Retina Project that is a consortium of five Department of Energy labs and four universities, as well as industry.

Yu-Chong Tai received his BS degree from National Taiwan University, and the MS and PhD degrees in electrical engineering from the University of California at Berkeley. He is currently a professor of Electrical Engineering and Bioengineering at the California Institute of Technology, and director of the Caltech Micromachining Laboratory. His current research interests include flexible MEMS, bioMEMS, MEMS for retinal implants, parylene-based integrated microfluidics, neuroprobes/neurochips, and HPLC based labs-on-a-chip.

Ellis Meng received her BS degree in engineering and applied science from the California Institute of Technology in 1997. She pursued her graduate studies in electrical engineering and received her MS in 1998 and PhD in 2003 at the same institution. She is now an assistant professor of Biomedical Engineering at the University of Southern California. In the National Science Foundation Biomimetic MicroElectronic Systems Engineering Research Center (BMES ERC) she is a Thrust Leader for Interface Technology and the Associate Director of Education and Student Diversity. She is a member of Tau Beta Pi, the American Society of Mechanical Engineers (ASME), the Society of Women Engineers (SWE), and the Association for Research in Vision and Ophthalmology (ARVO).